

ChemComm

Accepted Manuscript



This is an *Accepted Manuscript*, which has been through the Royal Society of Chemistry peer review process and has been accepted for publication.

Accepted Manuscripts are published online shortly after acceptance, before technical editing, formatting and proof reading. Using this free service, authors can make their results available to the community, in citable form, before we publish the edited article. We will replace this *Accepted Manuscript* with the edited and formatted *Advance Article* as soon as it is available.

You can find more information about *Accepted Manuscripts* in the [Information for Authors](#).

Please note that technical editing may introduce minor changes to the text and/or graphics, which may alter content. The journal's standard [Terms & Conditions](#) and the [Ethical guidelines](#) still apply. In no event shall the Royal Society of Chemistry be held responsible for any errors or omissions in this *Accepted Manuscript* or any consequences arising from the use of any information it contains.

COMMUNICATION

A ratiometric fluorescent molecular probe for visualization of mitochondrial temperature in living cell

Cite this: DOI: 10.1039/x0xx00000x

Received 00th January 2012,
Accepted 00th January 2012

Mitsumasa Homma, Yoshiaki Takei, Atsushi Murata, Takafumi Inoue and

DOI: 10.1039/x0xx00000x

Shinji Takeoka*

www.rsc.org/

Mitochondrial thermodynamics is the key to understand cellular activities related to homeostasis and energy balance. Here, we report the first ratiometric fluorescent molecular probe (Mito-RTP) that is selectively localized in the mitochondria and visualize the temperature. We confirmed that Mito-RTP could work as a ratiometric thermometer in cuvette and living cell.

Cellular events and functions are performed by a series of chemical reactions that can be described in terms of thermochemistry. Living cells efficiently utilize these chemical reactions to produce the optimum temperature for biomolecular dynamics and enzymatic reactions. Furthermore, it is presumed that temperature variations must exist when metabolic activities vary e.g., at each stage of the cell cycle, between different kinds of cells, during environmental changes or when abnormal cells appear. Therefore, intracellular or subcellular thermometry is a potent analytical method for understanding molecular biological functions related to temperature. Recently, various types of fluorescent thermometers have been developed^{1,2}. Some thermometers, including polymer nanogels³, polymer dots^{4,5}, quantum dots⁷, nanodiamonds⁸, polymer nanoparticles^{9,10}, have high spatial resolution in cultured cells but their intracellular localization is difficult to control.

Uchiyama *et al*¹¹ recently constructed a polymer-based fluorescent thermometer and revealed that each organelle has a different temperature within the cell. Although this method can determine the temperature of each organelle, it could not avoid the effects of heat diffusion. Therefore, the importance of developing a direct organelle thermometry method was recognized. Kiyonaka *et al*¹² has also developed a genetically encoded fluorescent thermometer. The methodology is based on a temperature sensitive coiled-coil GFP and is capable of measuring the temperature of a targeted organelle directly. However, the technique is time consuming in terms of setting up the gene expression.

Department of Life Science & Medical Bioscience, Graduate School of Advanced Science & Engineering, Waseda University, TWins 2-2 Wakamatsu-cho, Shinjuku-ku, Tokyo 162-8480 (Japan). E-mail: takeoka@waseda.jp

By contrast, low molecular weight chemical probes are easy to handle for staining either cultured or primary cells. In addition, membrane permeability and intracellular localization of chemical probes can be controlled by their physicochemical properties¹³. However, the accuracy of single-molecule fluorescence imaging is limited to using moving cells and transported organelles because the fluorescence intensity is also influenced by the focus point. The ratiometric property is a powerful means of measuring activities within a living cell because this method can negate fluorescence changes related to the concentration of fluorophore or focus drift.

As far as we know, this is the first study to report a small molecular ratiometric thermosensor for organelles. In this paper, we selected mitochondria as the first targeted small organelle because it plays a key role in maintaining thermal homeostasis in the cell¹⁶.

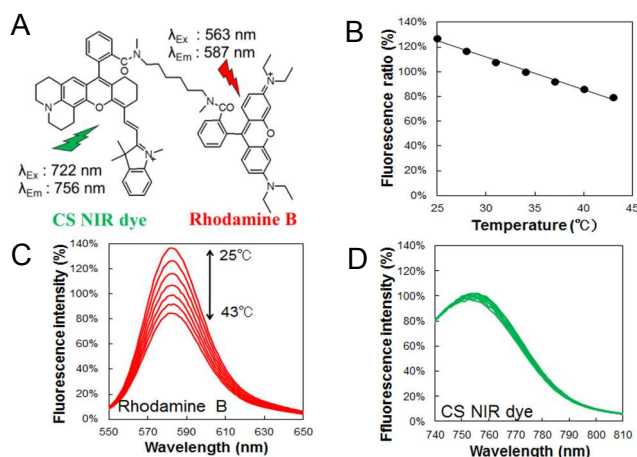


Fig. 1 *In vitro* evaluation of Mito-RTP in various parameters. (A) Chemical structure of Mito-RTP. Thermosensitive rhodamine B and thermoinsensitive CS NIR dye were conjugated to each end of the linker. (B) Fluorescence intensity ratio (Rhodamine B/CS NIR dye, calculated from peak intensities of rhodamine B and CS NIR dye) was determined at various temperatures (normalized at 34°C). Fluorescence spectra of (C) rhodamine B (λ_{ex} = 563 nm) and (D) CS NIR dye (λ_{ex} = 722 nm) measured with a spectrophotometer every 3°C from 25°C to 43°C.

Based on our previous technique⁹, we designed a mitochondria-targeting ratiometric temperature probe (Mito-RTP). Mito-RTP is composed of two kinds of rhodamine dyes; namely rhodamine B and CS NIR dye (Fig. 1A). The fluorescence intensity of rhodamine B decreased linearly with elevated temperature¹⁴. This property is due to the changes in ratio (photons emitted/photon absorbed), which depends on the rotation of diethylamino groups on the xanthen ring, resulting in the decrease in the quantum yield with increasing temperature. While, the fluorescence intensity of CS NIR dye¹⁵ was expected to be stable in various temperatures because the molecular rotation in this structure is restricted. These two fluorophores were coupled at each end of the hexamethylenediamine linker to provide a ratiometric property. Furthermore, due to their hydrophobicity, rhodamine fluorophores are known to readily pass through the cell membrane and specifically localize to the mitochondria¹⁶. In order to maintain the stability of Mito-RTP, amide bonds of the hexamethylenediamine linker were methylated to avoid forming the deprotonation inducing inter-molecular quenching state^{15,17}. Thus, Mito-RTP stains the intracellular mitochondria within a short period of time (<30 min) after simply adding the dye to the extracellular solution. The cells are then visualized in order to monitor the mitochondrial thermodynamics. As such, the technique is unaffected by changes to the focal point, concentration of the fluorophore, pH or ionic strength.

Mito-RTP was synthesized by 10 steps of organic chemical reactions. A full description of each reaction step is described in the *Supporting Information* (Fig. S1). Each compound was characterized by NMR and ESI-MS (Fig. S2 – S12). The fluorescence spectrum of Mito-RTP (Fig. S14) showed both absorption and emission wavelengths of the thermally sensitive rhodamine B and thermally insensitive CS NIR dye, which were well separated for dual fluorescence imaging.

Temperature sensitivity of Mito-RTP from 25°C to 43°C was evaluated in a cuvette with a spectrophotometer. As anticipated, the fluorescence intensity of rhodamine B reversibly responded to changes in temperature (Fig. 1C), whereas that of CS NIR dye was constant (Fig. 1D). The fluorescence intensity ratio of these two fluorophores (Rhodamine B/CS NIR dye, calculated from peak intensities of rhodamine B and CS NIR dye) showed a linear decline with increasing temperature (Fig. 1B, S15). From the slope of the linear fit, the thermal sensitivity of Mito-RTP was -2.65%/°C. Within living cells, conditions such as pH and ionic strength vary between locations and with time. Fluorescent thermometers should be insensitive to such environmental parameters. In our Mito-RTP, the fluorescence intensity ratio did not change when the pH was varied between 4 and 10 (Fig. S16A) and ionic strength between 0 and 500 mM KCl (Fig. S16B). These results indicate that Mito-RTP has a ratiometric property with temperature. In addition, methylation of the hexamethylenediamine linker prevents formation of the quenching state of rhodamine fluorophores. This gives a stable fluorescence property against environmental parameters within the physiological range.

We then confirmed that Mito-RTP at a 1 μ M concentration within a cancer cell line (HeLa cells). 1 μ M Mito-RTP displayed no significant cytotoxicity (Fig. S18) and this concentration was used for all the HeLa cell experiments. The localization of Mito-RTP was observed from the fluorescence intensity of rhodamine B and CS NIR dye with mito-tracker green. The fluorescence images of both rhodamine B in Mito-RTP (Fig. 2A left) and mito-tracker green (Fig. 2A center) were

completely merged (Fig. 2A right). These observations indicated that Mito-RTP was easily able to permeate the cell membrane owing to its hydrophobicity and that 30 min incubation was sufficient time to stain the mitochondria.

We also evaluated the effect of defocusing on the fluorescence intensity ratio because mitochondria are transported in any direction by motor proteins¹⁸. Fluorescence intensities of both rhodamine B and CS NIR dye showed a maximal value at $z = 0$, where cells were in focus, and decreased by defocusing as the objective lens moved up and down from $z = 0$. The fluorescence intensity ratio, however, remained constant, demonstrating the advantage of a ratiometric measurement (Fig. 2B).

We further evaluated the temperature sensitivity of Mito-RTP localized in mitochondria by observing the temperature-dependent fluorescence intensities. The temperature of the extracellular buffer was controlled from 34°C to 41°C (0.5°C/5 min) using a stage incubator and measured with a digital thermocouple having an accuracy of $\pm 0.1^\circ\text{C}$. The fluorescence intensities of rhodamine B (Fig. 2C) and CS NIR dye (Fig. 2D) during gradual heating were scattered due to the focus drift along the z -axis. However, a linear decline in the fluorescence intensity ratio (rhodamine B/CS NIR dye) was clearly observed as the extracellular temperature increased ($r = -0.808$, $P = 1.10 \times 10^{-88}$ by a Pearson's correlation coefficient test) (Fig. 2E). The slope of the linear fit for the average values was -2.72%/°C. The accuracy of the temperature measurement was determined to be 0.6°C.

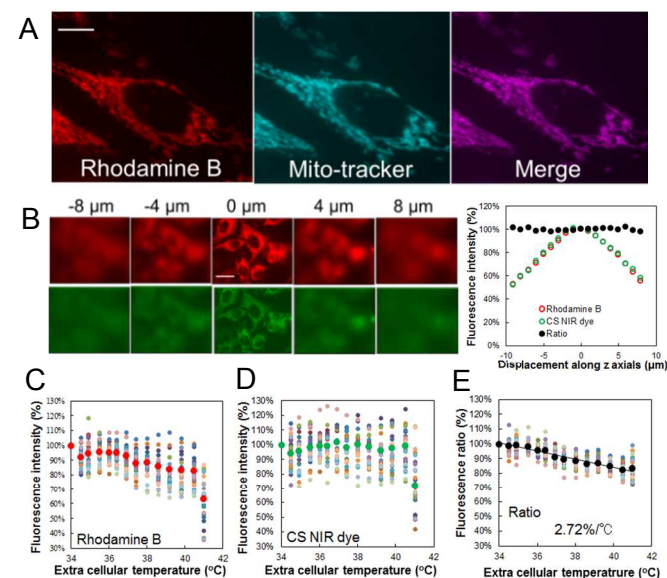


Fig. 2 Evaluation of Mito-RTP properties with a conventional fluorescence microscope. (A) Localization of Mito-RTP in living HeLa cells. Fluorescence images of rhodamine B in Mito-RTP (Left), mito-tracker green (center) and their merged images (right). Scale bar indicate 5 μm . (B) Focus independent fluorescence ratio of Mito-RTP. Fluorescence images of rhodamine B (red) and CS NIR dye (green) at each focus point (Left) Scale bar indicate 20 μm . Fluorescence intensities of both rhodamine B (red) and CS NIR dye (green) approached the maximum at $z = 0$ and decreased with defocusing, whereas the fluorescence ratio (black) was always constant (Right). Fluorescence intensities of (C) rhodamine B (average values shown in red) and (D) CS NIR dye (average values shown in green) under gradual heating from 34°C to 41°C (E) fluorescence intensity ratio (average values shown in black). The linear fit of the average values of the fluorescence intensity ratio indicate that thermal sensitivity was -2.72%/°C ($r = -0.808$, $n = 26$ ROIs, $P = 1.1 \times 10^{-88}$ by Pearson's correlation coefficient test).

It was concluded that the ratiometric measurement of Mito-RTP could appropriately compensate the focus drift caused by cellular movement and transportation of mitochondria inside the cell. As such, Mito-RTP generates a temperature-dependent fluorescence change in mitochondria within living HeLa cells.

The utility of Mito-RTP as a mitochondrial thermosensor was examined by monitoring mitochondrial temperature changes induced by external chemical stimuli using HeLa cells. We applied carbonyl cyanide 4-(trifluoromethoxy) phenylhydrazone (FCCP), which transports protons across the mitochondrial inner membrane, to prevent the coupling of ATP synthesis and oxidative phosphorylation, leading to heat generation^{12, 19, 20, 21}. Fluorescence intensities of rhodamine B (Fig. 3A) and CS NIR dye (Fig. 3B) in Mito-RTP were widely distributed because each region of interest (ROI) (N = 5 cells, n = 19 ROIs) detected signals from a different focus point. The fluorescence intensity ratio, however, showed a gradual decrease from around 150 seconds after addition of FCCP (Fig. 3C), but was constant for the DMSO control (Fig. 3D). The observed time lag (t = 0 to 150 s) is thought to be due to the diffusion time of FCCP, which was added dropwise to the extracellular buffer. The fluorescence intensity ratio of FCCP treated cells (t = 330) significantly decreased compared with that of the DMSO control cells (t = 330) ($P = 3.7 \times 10^{-5}$ by student's *t*-test) (Fig. 3E). Fluorescence ratio images (Fig. 3G) indicated that the heterogeneous temperature elevation in FCCP treated cells (t = 330) compared with untreated cells (t = -90) ($P = 8.1 \times 10^{-5}$ by student's *t*-test) (Fig. 3F). Mitochondrial temperature distribution within a cell has already been reported by the other published works^{6, 12}. Therefore, Mito-RTP is considered to monitor the FCCP-coupled heterogeneous thermogenesis in mitochondrial.

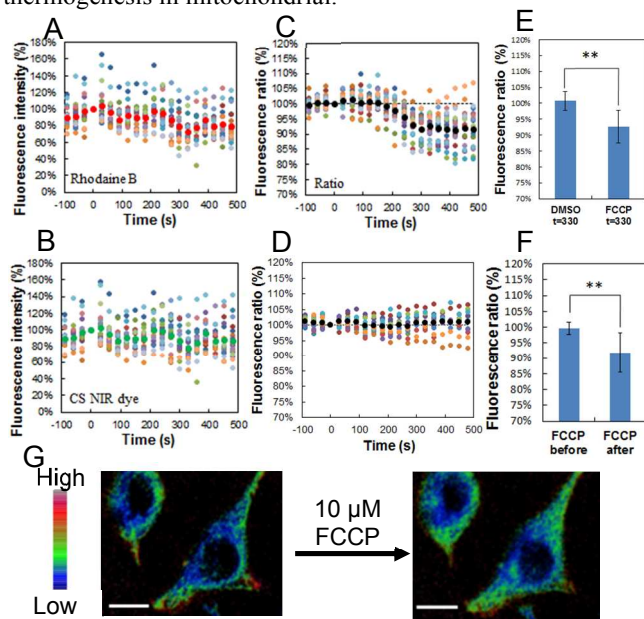


Fig. 3 Visualization of mitochondrial temperature in HeLa cells in the presence of 10 μM FCCP. Time course fluorescence signals of (A) rhodamine B (average values shown in red) and (B) CS NIR dye (average values shown in green), (C) fluorescence intensity ratio (average values shown in black) (N = 5 cells, n = 19 ROIs). (D) Normalized fluorescence ratio was obtained by applying 0.1% DMSO as control (average values in black) (n = 12 ROIs). (E) Student's *t*-test of DMSO and FCCP at t = 330s (** $P = 3.7 \times 10^{-5}$). (F) Student's *t*-test before (t = -90) and after (t = 330) addition of FCCP (** $P = 8.1 \times 10^{-5}$). (G) Ratio images (rhodamine B/CS NIR dye) before (t = -90) and after (t = 330) addition of FCCP. Scale bar indicate 10 μm .

In conclusion, we have successfully constructed a ratiometric fluorescent chemical thermosensor, which specifically localizes to mitochondria in a relatively short time period (< 30 min). We confirmed that Mito-RTP could work as a thermosensor both *in vitro* and in living cells. Ratiometric measurement using Mito-RTP was able to negate the effects of defocusing along the z-axis caused by cellular movements and concentration changes in the fluorophore. This novel system enabled us to visualize the FCCP-coupled temperature elevation in the mitochondria within HeLa cells. Mitochondrial thermodynamics plays a key role in cellular activities related to homeostasis and energy balance. Therefore, Mito-RTP is a powerful tool for analyzing how mitochondria activate in living cells. We believe this technique will provide information concerning the relationship between cellular activities and changes in temperature.

We thank Dr. H. Nakamura (Waseda U.), Prof. E. Latz (Bonn U.) and Dr. G. Horvath (Bonn U.), Prof. S. Ishiwata (Waseda U.), Dr. K. Oyama (Waseda U.) and Dr. S. Arai (WABIOS) for microscopic experiments and technical advices. This work was supported by Waseda U. Grant for Special Research Project and the JSPS Core-to-Core Program.

Notes and references

- C. D. S. Brites, P. P. Lima, N. J. O. Silva, A. Millan, V. S. Amaral, F. Palacio, L. D. Carlos, *Nanoscale*, 2012, **4**, 4799–4829.
- T. Ozawa, H. Yoshimura, S. B. Kim, *Anal. Chem.*, 2013, **85**, 590–609.
- C. Gota, K. Okabe, T. Funatsu, Y. Harada, S. Uchiyama, *J. Am. Chem. Soc.* 2009, **131**, 2766–2767.
- F. Ye, C. Wu, Y. Jin, Y. -H. Chan, X. Zhang, D. T. Chiu, *J. Am. Chem. Soc.* 2011, **133**, 8146–8149.
- P. J. Wu, S. Y. Kuo, Y. C. Huang, C. P. Chen, Y. H. Chan, *Anal. Chem.* 2014, **86**, 4831–4839.
- J. S. Donner, S. A. Thompson, M. P. Kreuzer, G. Baffou, R. Quidant, Mapping Intracellular Temperature Using Green Fluorescent Protein. *Nano Lett.* 2012, **12**, 2107–2111.
- C. H. Hsia, A. Wuttig, H. Yang, *ACS Nano*, 2011, **5**, 9511–9522.
- G. Kuksko, P. C. Maurer, N. Y. Yao, M. D. Lukin, *Nature*, 2013, **500**, 54–58.
- Y. Takei, S. Arai, A. Murata, S. Takoeka, *ACS nano*, 2014, **8**, 198–206.
- K. Oyama, M. Takabayashi, Y. Takei, S. Arai, S. Takeoka, S. Ishiwata, M. Suzuki, *Lab Chip.*, 2012, **12**, 1591–1593.
- K. Okabe, N. Inada, C. Gota, Y. Harada, T. Funatsu, S. Uchiyama, *Nat. Commun.*, 2012, **3**, 1–9.
- S. Kiyonaka, T. Kajimoto, R. Sakaguchi, D. Shinmi, M. Omatsu-Kanbe, H. Matsuura, H. Imamura, T. Yoshizaki, I. Hamachi, T. Morii, Y. Mori, *Nature* 2013, **10**, 1232–1240.
- S. Arai, S. C. Lee, D. Zhai, M. Suzuki, Y. T. Chang, *Scientific Reports*, 2014, **4**, 1–6.
- C. E. Estrada-Pérez, Y. A. Hassan, S. Tan, *Rev. Sci. Instrum.* 2011, **82**, 074901.
- L. Yuan, W. Lin, Y. Yang, H. Chen, *J. Am. Chem. Soc.* 2012, **134**, 1200–1211.
- L. V. Johnson, M. L. Walsh, L. B. Chen, *Cell Biology*, 1980, **77**, 990–994.
- X. Qian, Y. Xiao, Y. Xu, X. Guo, J. Qiana, W. Zhua, *Chem. Commun.*, 2010, **46**, 6418–6436.
- D. A. Rube, A. M. van der Blik, *Mol. Cell Biol.*, 2004, **256/257**, 331–339.
- A. Bartelt, O. T. Bruns, R. Reimer, H. Hohenberg, H. Itrich, K. Peldschus, M. G. Kaul, U. I. Tromsdorf, H. Weller, C. Waurisch, A. Eychmüller, P. L. S. M. Gordts, F. Rinninger, K. Bruegelmann, B. Freund, P. Nielsen, M. Merkel, J. Heeren, *Nature Med.*, 2011, **17**, 200–206.
- M. A. Paulik, R. G. Buckholz, M. E. Lancaster, W. S. Dallas, E. A. Hull-Ryde, J. E. Weil, J. M. Lenhard, *Pharm. Res.*, 1998, **15**, 944–949.
- H. Terada, *Biochim. Biophys. Acta.*, 1981, **639**, 225–242.